

**2018 NDIA GROUND VEHICLE SYSTEMS ENGINEERING AND TECHNOLOGY
SYMPOSIUM
MATERIALS & ADVANCE MANUFACTURING (M&AM) TECHNICAL SESSION
AUGUST 7-9, 2018 - NOVI, MICHIGAN**

FORMING AND WELDING INNOVATIONS FOR ARMOR STEELS

**John Lawmon,
American Engineering
& Manufacturing Inc,
Elyria, OH.**

**Boian Alexandrov,
The Ohio State
University, Columbus,
OH**

**Matthew Duffey.
Tiffany Ngan.
Bryan Cheeseman, Army Research Laboratory,
MD.**

ABSTRACT

This paper reviews research that has been conducted to develop inductively assisted localized hot forming bending technologies, and to use standardized welding tests to assess the practicality and potential benefits of adopting stainless based consumables to weld both existing and evolving armor alloys.

For the titanium alloy Ti6Al4V it was determined that warming the plate to circa 600°F would improve the materials ductility (as measured by reduction of area) from ~18 to 40% without exposing the material to a temperature at which atmospheric contamination would be significantly deleterious.

For the commercial alloy BB and class 1 armor alloy it was found that there was little effect on the charpy impact toughness and the proof strength as a result of processing at 900 °F with either air cool or water quench and there was an added benefit of lower residual stresses in the finished bends compared to cold formed bends. Heating “alloy BB” to 1600 °F followed by water quench resulted in mechanical properties that were equivalent to those of the parent plate with the exception of a strip of material in the transition hot zone whose temperature, before quench, was between 900 °F and 1600 °F. Heating class 1 armor to 1600°F followed by water quench increased the ultimate tensile strength.

Further work is recommended for alloy BB and class 1 armor, using a higher induction power, to determine how narrow the transition hot zone, in which lower charpy impact toughness was noted, can be made.

The weldability study indicated that grade 309LHF stainless steel is the least likely to crack when making single pass welds in “alloy BB”. It was not possible to make a similar assessment based on the available data for the class 1 RHA when using stainless steel consumables. When using ferrous consumables it was apparent that preheat was beneficial and that LA100 performed better than ER70S-6. It is recommended that the weldability study be repeated with a statistically significant number of Tekken or restrained T joint solidification cracking tests at different travel speeds to examine the significance of weld bead profile.

INTRODUCTION

This paper will review two elements of research and innovation associated with the hot forming, and welding of armor alloys.

Firstly, it will consider how the use of inductively assisted hot bending technologies for titanium alloy and armor steels can be used as a direct alternate to both welding and cold forming to reduce production costs and provide an incremental improvement to armored vehicle performance and crew safety.

Secondly, it will examine the weldability data, for a range of weld consumables, that was obtained with standardized testing for both traditional rolled homogenous armor and a widely used low alloy steel armor.

Inductively assisted hot forming Ti6Al4V

The objectives of this task were to scientifically underpin and build inductively assisted hot forming tooling to:

- Form titanium alloy gunner protection kits.
- Form thick steel armor.

For the gunner protection kits titanium alloy Ti6Al4V was selected as a relatively low-density armor material that could be retrofitted around roof top gun mounts to provide increased crew protection. A particular benefit of this material was its high yield strength and relatively low elastic modulus, compared to steel, which allows it to support large elastic strains and hence provide good ballistic performance with the added benefit of low density to minimize additional “top weight”.

A range of designs, for multiple platforms, required several panels to form a protective ring around the gunner. These panels could have been welded together, however innovative thinking proposed that the panels be cut from a single flat plate and bent to shape, thus: eliminating expensive and time-consuming welding; simplifying quality control; reducing the part count and number of drawings; simplifying logistics and handling.

Previous work with the bend testing of Ti6Al4V welds has shown that when the ductility limit is surpassed the stored energy will be released as a fast fracture with unrestrained parts able to fly dangerously in an unpredictable and unacceptable manner. It was subsequently theorized that the bent material was subjected to a previously unrecognized load, caused by friction between the material and die set, that results in an outer fiber elongation that is higher than predicted by the simplified equation below which does not consider neutral axis shift.

Percentage elongation = $100 * t / [(2 * r) + t]$ where r = bend radius and t = material thickness.

This knowledge was carried forward into production bend tooling equipped with roller dies to reduce the frictional drag.

Existing literature [1] provided ductility data (bend factors) for many titanium alloys however the grade selected for this program is subtly different and a program of work was undertaken at Ohio State University (OSU) [2], [3] to examine the alloys’ high temperature properties using both large tensile test frames and the Gleeble thermal simulator at different strain rates. The results of these Gleeble tests, summarized in Figure 1 and Figure 2, show there is only a small change in the reduction of area as a result of straining at either 1 or 10mm/s.

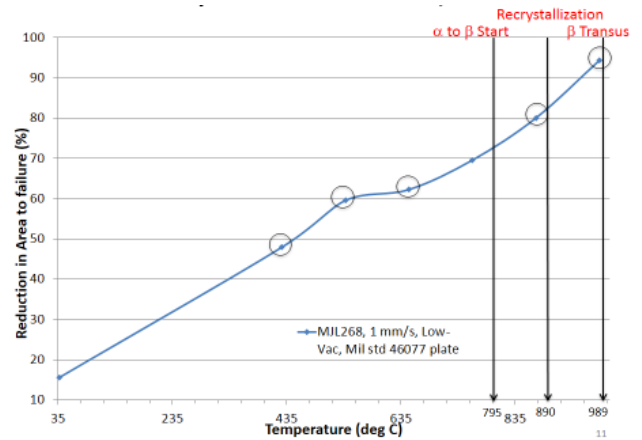


Figure 1: Plot of Reduction-in-Area (RA) vs Temperature for Ti-6Al-4V Class 1 plate at 1 mm/s extension rate

FORMING AND WELDING INNOVATIONS FOR ARMOR STEELS.

John Lawmon et al.

Approved for public release; distribution is unlimited.

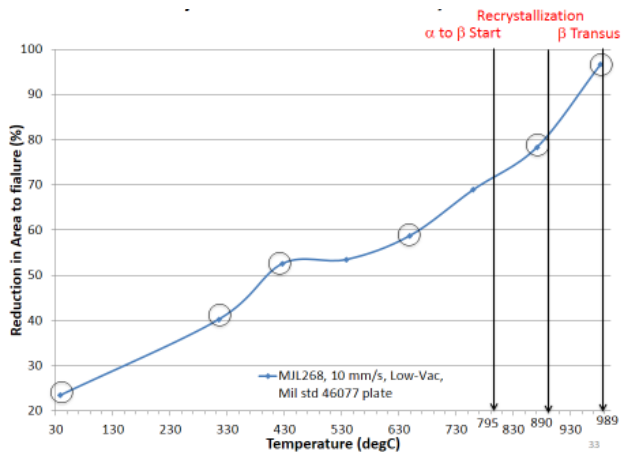


Figure 2: Plot of RA vs Temperature for Class 1 plate at 10 mm/s extension rate

There is thus a relationship between the material's ductility and safe bend radius that are design limitations. Recognizing that the existing design bend radius would provide only a small factor of safety during production two changes were made to improve formability: 1) The press brake tooling was changed to allow the use of a roller die bed to reduce the frictional component. 2) The bend line was flame preheated, immediately before forming, to take advantage of the alloys increased ductility at higher temperatures. These changes were both successfully implemented, however it was recognized that the gas fired pre-heating was operator sensitive and a potential source of undesirable brittle alpha case on the surface should the plate be locally overheated. Further innovation led to the design, development and testing of the single sided induction heating system shown in Figure 3, able to heat the material to a controlled temperature. A particular benefit of this system is its ability to quickly heat the material to the required forming temperature of ~ 600°F where the ductility increased from ~18 to 40%. In addition to providing a rapid controlled process there is the added benefit that the ductility improvement has been achieved at a modest temperature where diffusion of deleterious oxygen and nitrogen is relatively slow.



Figure 3: Single sided induction table and 3 bend part

An example of a completed and field-tested turret formed with this system is shown in Figure 4.



Figure 4: Turret success

Inductively assisted hot forming of Armor Steel

From the prior work a natural extension was to determine whether the same principals could be used to advantageously form thicker heat-treated armor steels with more complex metallurgies whose composition and properties are shown in Table 1.

FORMING AND WELDING INNOVATIONS FOR ARMOR STEELS.

John Lawmon et al.

Approved for public release; distribution is unlimited.

Table 1: Composition of class 1 RHA and “alloy BB” steel plates

Element (wt%)	RHA Class 1* (MJL478)	Commercial Armor (Alloy BB) (MJL469)
Carbon	0.26	0.19
Manganese	1.31	0.85
Si	0.28	0.22
Ni	0.06	1.91
Cr	0.06	0.6
Mo	0.45	0.586
0.2% Proof	162ksi	168ksi
UTS	169ksi	208ksi
Hardness	260 to 300Hv 10kg (specification)	~480Hv 10kg (specification)
Charpy	47 to 75J @ -40°C (specification)	~80J @ -40°C (specification)

To examine this possibility a project was established with OSU to develop technical data. This program included a literature review and the use of a Gleeble thermal simulator, light radiation furnace and traditional metallurgical techniques.

The Gleeble thermal simulator was used to determine the high temperature properties of “alloy BB”. As expected this work, which is summarized in Table 2, shows how the materials ductility steadily increases with temperature.

Table 2: Reduction in area vs test temperature for hot ductility testing of “alloy BB” with the Gleeble thermal simulator

Testing temperature °C	Reduction in area (%)
300	58
350	78
400	80
450	81

The research conducted using the light radiation furnace (“alloy BB”) developed the relationship shown in Figure 5 between Vickers hardness and time at temperature (seconds and degrees Kelvin respectively) as represented by the Hollomon-Jaffe

parameters. This work indicated that when the alloy is heated to 1200°F for approximately one minute and air cooled that there will be loss of ~150HV that is analogous to heating for 20 minutes at 1100°F.

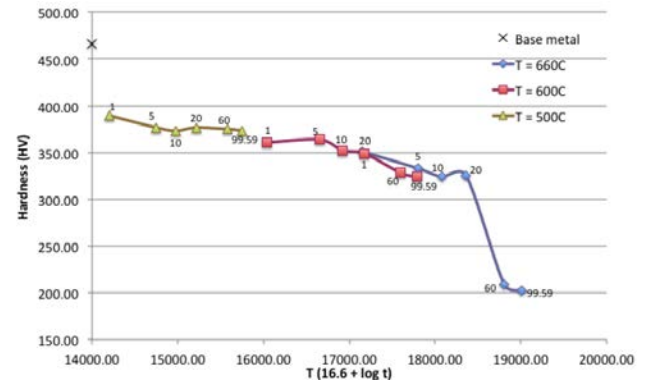


Figure 5: Vickers hardness vs Hollomon Jaffe Parameter for “alloy BB”

In parallel with this work at OSU a small research machine (Figure 6) was designed and constructed at American Engineering & Manufacturing (AEM) to allow whole plate samples to be heated and formed. A video of the system heating and forming “alloy BB” plates can be viewed at <https://youtu.be/PABkiOdlh7s>



Figure 6: Hydraulic press and oscillating induction station

To provide a set of benchmark data “alloy BB” bends JT3 & JT4 were cold formed for comparison

against hot formed bends KG167 and KG168 using the conditions listed in Table 3. Figure 7 & Figure 8 show a typical plot of the data captured using our integrated Allen-Bradley “Factory Talk” software for the hot bends. From this data it can be seen that forming at 1600°F reduces the required load by a factor of 7.8 compared to forming at 900°F.

Table 3: Bend parameters

Bend	Temperature	Induction power	Hydraulic pressure	Ram speed	Number of coil oscillations
JT3	74°F				
JT4	74°F				
KG167	900°F	25%	107 bar	2.2mm/sec	3
KG168	1600°F	35%	13.6 bar	1.8mm/sec	7

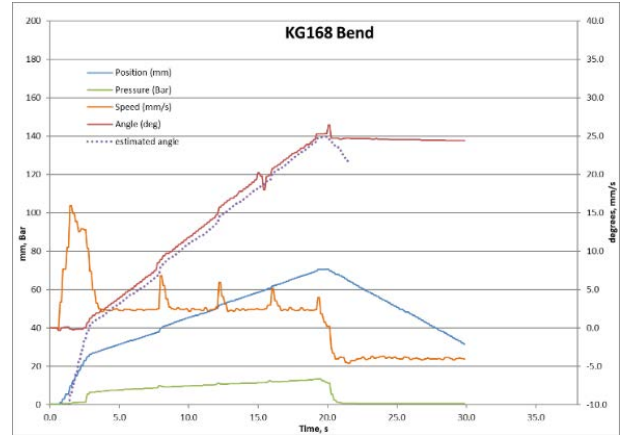


Figure 8: Data log for bend KG168

The bends were subsequently analyzed non-destructively and destructively for cracking the nature of the residual stress field and the through thickness hardness.

Visual examination of a similar cold bend JT5 (Figure 9) made with the bend line parallel to the principal rolling direction indicated fine surface crazing. Subsequent microscopic examination (Figure 10) revealed a martensitic microstructure with a decarburized surface layer (not shown in micrograph) that was intermittently cracked.

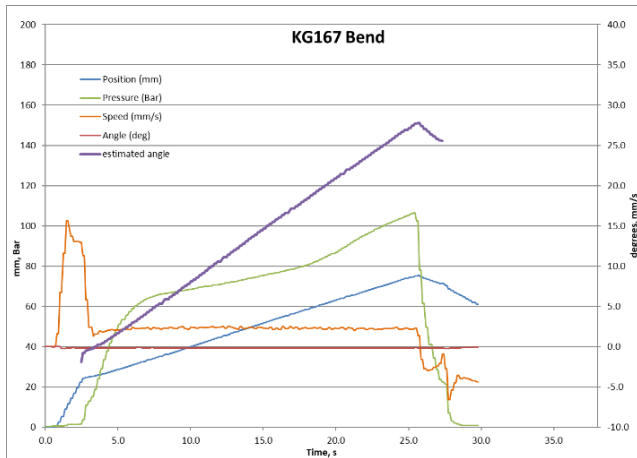


Figure 7: Data log for bend KG167

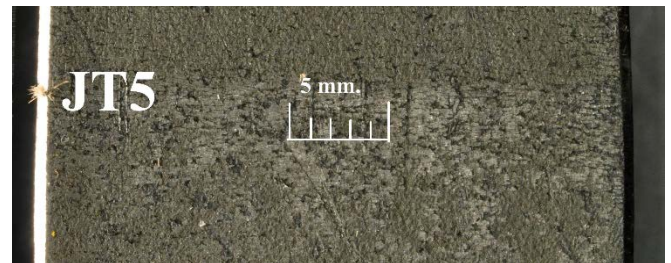


Figure 9: Outer surface of cold formed bend JT5



Figure 10: Cross section through bend JT5 remote from the surface

Examination of the longitudinal residual stress data shown in Figure 11 confirms that the longitudinal residual stress decreases with temperature and that plates formed at 1600°F [870°C] will have outer fiber residual stresses some 6 times lower than those of cold formed bends of similar geometry. This temperature is clearly above the temper temperature of the base material and some potentially adverse changes in the microstructure would be anticipated.

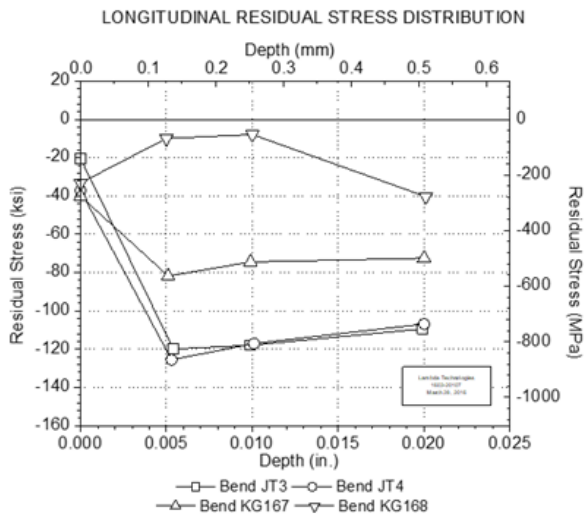


Figure 11: Longitudinal residual stress distribution

The results of a 10 kg Vickers hardness survey, conducted to obtain a 1st indication of this change

are shown in Figure 12 where it can be seen that both of the cold formed bends have undergone strain hardening which is most noticeable at the outer and inner surfaces compared to the parent plate. Both of the hot bends have softened, with the greatest softening occurring in bend KG168 which was heated to 1600°F, and like KG167 (which was heated to 900°F), allowed to air cool.

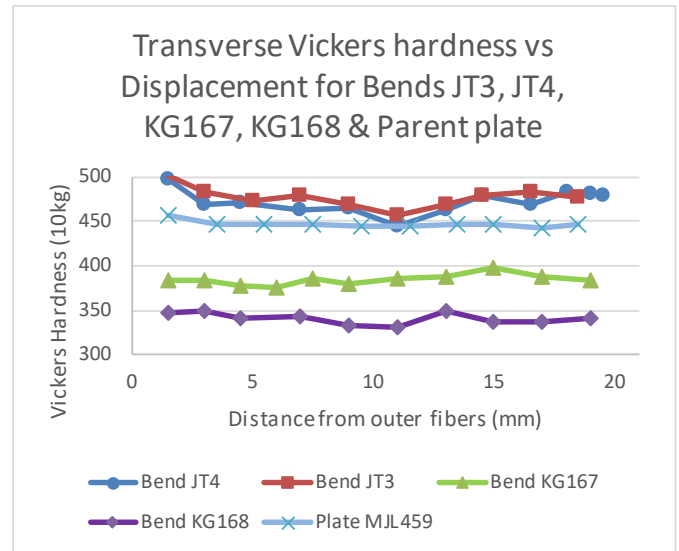


Figure 12: Transverse Vickers hardness survey for cold and hot formed bends

Microstructural examination of both KG167 and KG168 (formed at 900°F and 1600°F respectively) reveals a decarburized surface layer with Carbide

precipitates in a ferritic microstructure immediately below as shown in Figure 13.



Figure 13: Image close to the surface of bend KG167

The structure at the center of the plate was believed to be either pearlite or bainite (Figure 14) but it was not possible to definitively resolve the structure at 1000x magnification.



Figure 14: Image close to the mid thickness of bend KG167

Examination of the microstructure of as received plate reveals a simialry decarburized surface layer with carbide precipitates in a ferritic microstructure, and a martensitic microstructure (Figure 15) in the remainder of the plate.



Figure 15: Image at mid thickness of as received plate

By comparing these different microstructures it appears that the observed surface decarburization and carbide precipitates are associated with the manufacture of this plate and that the application of induction heating followed by air cool from both 900°F and 1600°F has normalized the bulk plate.

Recognizing that the objective of the project was to develop an efficient process that replaces welding and provides a final structure with properties equal to or better than a weld, it was decided to build the machine shown in Figure 16 that is able to heat and form 48" wide plates of 20 mm thick material from which additional hardenss data plus tensile and impact coupons could be taken in both the transverse and longitudinal directions.



Figure 16: 175 ton press brake and induction coils for 20 mm plate

Using both the small development machine and the larger machine a test matrix (Table 4) was developed and completed for a commercial alloy (designated “Alloy BB”) and rolled homogenous armor (RHA) to MIL46077 class 1) to include air cooling and water quenching.

Table 4: Test matrix for armor steel plates

Base material	900°F air cool	900°F water quench	1600°F air cool	1600°F water quench
Alloy BB	KG232 KG172			
Alloy BB		KG223		
Alloy BB			KG233 KG171	
Alloy BB				KG222
RHA	KG230			
RHA		KG226		
RHA			KG231	
RHA				KG227

For KG172 and KG171 the coupons were cut from a plate 24” long x 12” wide, and for KG226, KG227, KG2230, KG231, KG222, KG223, KG232 and KG233 they were cut from a 48” wide x 60” long plate.

Macro/hardness, tensile and charpy coupons were removed in accordance with Figure 17 and Figure 18 to provide mechanical properties within the hot

zone, at the edge of the hot zone and in the parent material. Figure 19 shows one of the large plates after removal of the coupons.

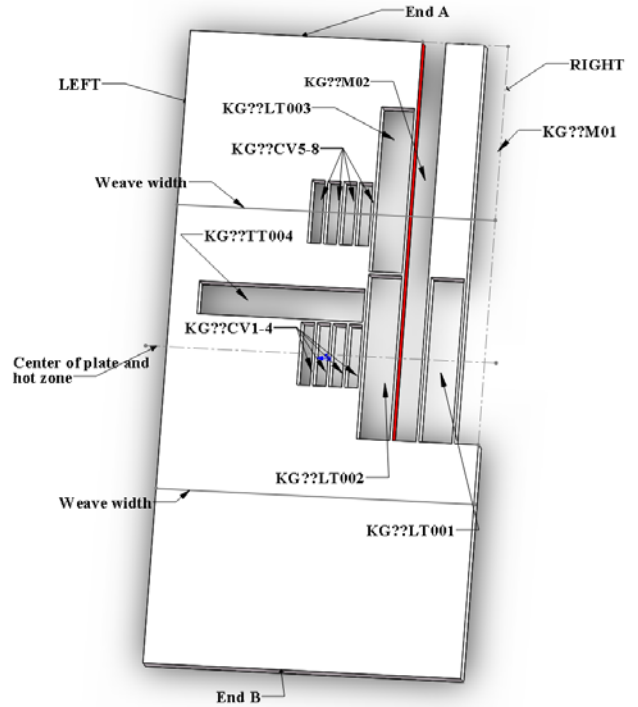


Figure 17: Cutting plan for KG172 and KG171

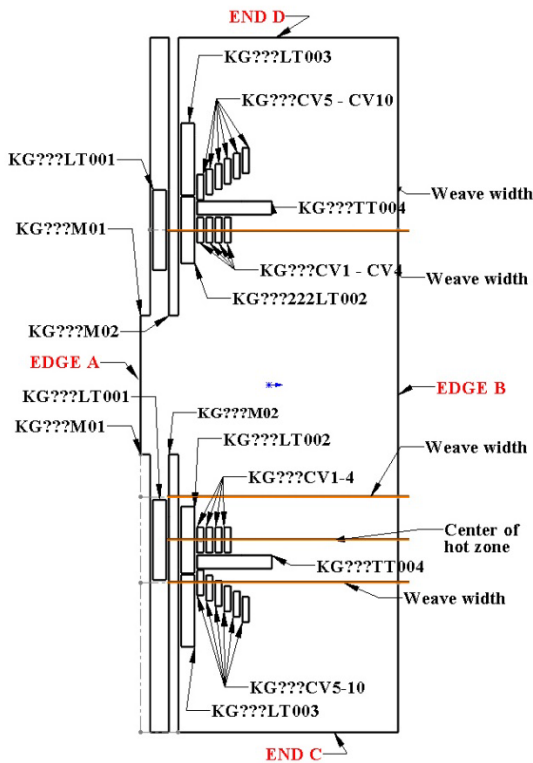


Figure 18: Cutting plan for 60" x 48" plates



Figure 19: Armor plate after removal of test coupons

“Alloy BB”

The hardness surveys for the 2' long x 1' wide “alloy BB” plates KG172 (Figure 20) and KG171 (Figure 21), show a reduction in hardness from the cooler plate end towards the center of the hot zone with the lowest levels of hardness being observed in the plate heated to 1600°F and air cooled. The hardness of both plates was measured as circa 400 Vickers at the ends indicating that the whole of the macro section may have been affected as the parent plate hardness is ~440 Vickers. It should be noted that induction heating causes a dog bone heat path as shown schematically in Figure 22 and on the machine in Figure 23 and hence the hot zone is wider at the plate edge than in the middle of the plate.

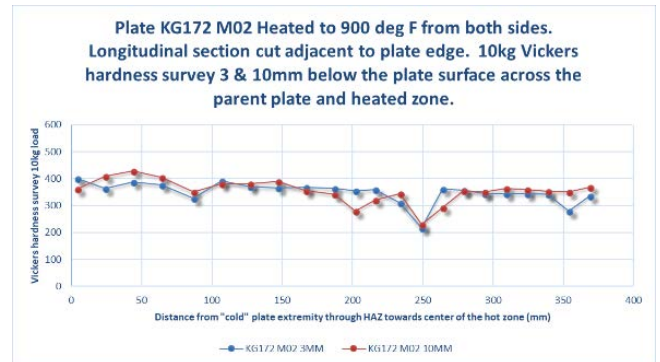


Figure 20: Hardness survey for “alloy BB” plate KG172 treated at 900°F with air cool

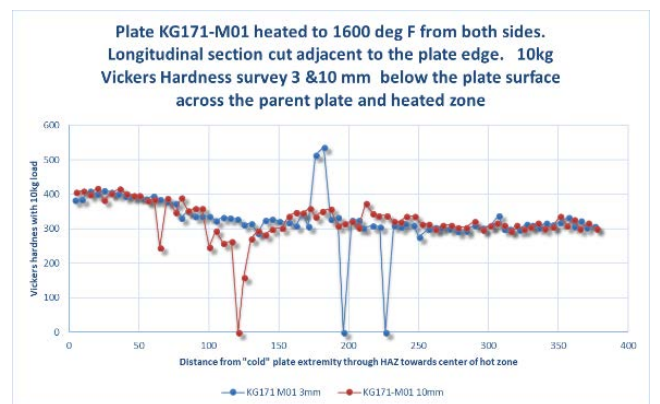


Figure 21: Hardness survey for “alloy BB” plate KG171 at 1600°F with air cool

FORMING AND WELDING INNOVATIONS FOR ARMOR STEELS.

John Lawmon et al.

Approved for public release; distribution is unlimited.

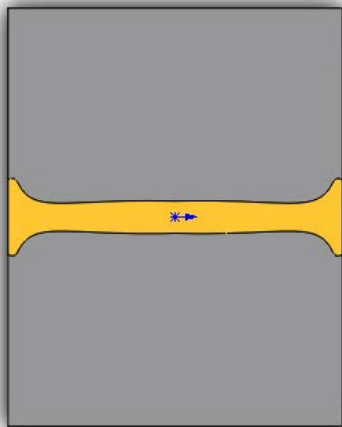


Figure 22: Induction heating dog bone edge effect



Figure 23: Small plate showing edge effect

The hardness surveys for the larger (5' x 4') “alloy BB” plates are shown in Figure 24 and Figure 25.

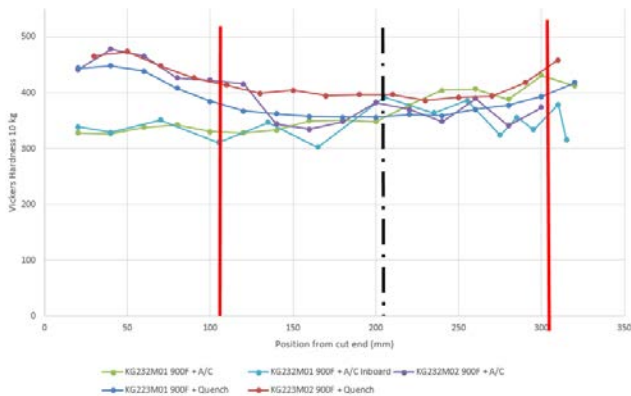


Figure 24: Hardness survey for “alloy BB” plates at 900°F with and without water quench

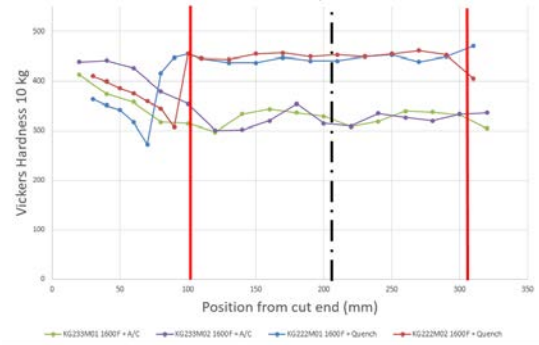


Figure 25: Hardness survey for “alloy BB” plates at 1600 °F with and without water quench

For the “alloy BB” macro KG232-01 (Note:- The 01 suffix for macro sections were cut adjacent to the plate edge and therefore include more of the dog bone heating effect than 02 suffix macro sections which were cut approximately 60 mm away from the plate edge) shows similar hardness results to those measured in KG172 formed at 900 °F with air cooling at the plate edge with softening throughout and the lowest hardness measured in the center of the hot zone.

Data from macro section KG232-M02, at the same temperature but cut further away from the plate edge, confirms the dog bone effect as its measured hardness is higher at the cold end.

For the “alloy BB” plate KG223 which was heated to 900°F and water quenched, the reduction of hardness is much smaller and of the order of 40 points, except for a region 50 mm beyond the weave width where it increases to 480 Vickers (irrespective of distance from the plate edge).

The “alloy BB” plate (KG233) heated to 1600°F and air cooled shows an approximately 140 points drop in hardness. The “alloy BB” plate KG222) heated to 1600°F and water quenched hold its hardness at circa 440 Vickers except for a 75 mm wide region beyond the directly heated zone where the hardness drops ~150 points. This softer zone appears to coincide with the previously noted dog bone hot zone present at the plate edge. On the one hand this dog bone effect is concerning because of the implications for mechanical properties however it does broaden the hot zone at the plate edge where

cracks are known to initiate during cold forming and thus it has some beneficial effect.

The tensile test results for the “alloy BB” plates are shown in Table 16. For both the small and large “alloy BB” plates (KG172 & KG232) heated to 900°F followed by air cooling, and KG223 heated to 900°F followed by water quench, the 0.2% proof stress is largely unchanged and the UTS drops between 20 and 30 ksi compared to the as received parent plate.

For the “alloy BB” plates (KG171 & KG233) heated to 1600°F followed by air cool, both the 0.2% proof stress and UTS drop by approximately 50 ksi compared to the as received parent plate.

For the “alloy BB” plate heated to 1600°F (KG222) followed by water quench, the 0.2% proof stress and UTS are both similar to the as received parent material.

The Charpy impact data for “alloy BB” plates are summarized in Table 5.

Table 5: Charpy impact test results for "Alloy BB plates"

Commercial Armor (Alloy BB)						
Coupon	Treatment	Sample location and Cv -40C (Joules)				
		1	2	5	7	10
Parent	As received					80
KG172	900°F + Air cool		74	70		
KG232	900°F + Air cool	96	114	127	65	108
KG223	900°F + Quench	87	108	95	106	100
KG171	1600°F + Air cool		28	24		
KG233	1600°F + Air cool	22	16	16	16	103
KG222	1600°F + Quench	103	103	27	168	106
Location 1 is at the center of the hot zone						
Location 2 is at the center of the hot zone						
Location 5 is approximately on the maximum induction coil oscillation line						
Location 7 is approximately 25mm beyond location 5mm						
Location 10 is approximately 63mm beyond location 5						

For “alloy BB” plates both the 900°F air cooled (KG172 & KG232) and 900°F + water quench (KG223) impact toughness’ compare favorably with the parent plate at all of the locations tested.

The plates KG171 and KG233 that were air cooled from 1600°F have not responded well and the Charpy impact values are poor. The plate KG222 that was water quenched from 1600°F has good Charpy impact properties except at location 5 (approximately on the weave line) and it was first thought that this corresponds with the locally low hardness noted above however subsequent hardness testing of the Charpy impact coupons shows a hardness of 350 Vickers on one side and 500 on the other. It therefore follows that no definitive conclusions can be drawn between the impact toughness and Vickers hardness without further microstructural examination and a more detailed hardness traverse.

Class 1 RHA

The hardness plots for the class 1 RHA plates are shown in Figure 26 and Figure 27 and the estimated travel of the induction coil is represented by the red lines which are based on an assumed midpoint that may be too far left.

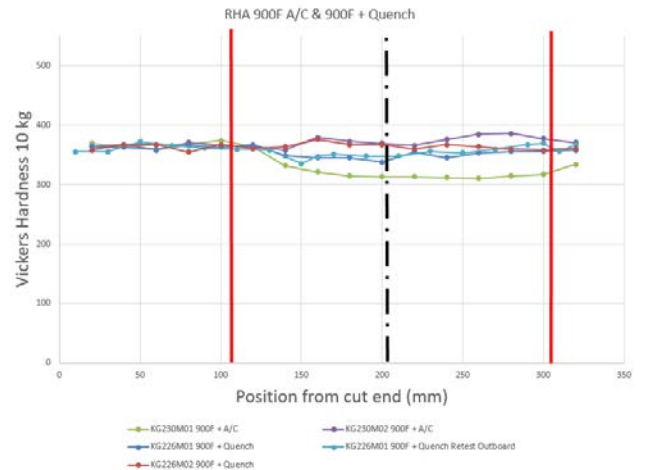


Figure 26: Hardness survey for class 1 RHA plates at 900°F with and without water quench

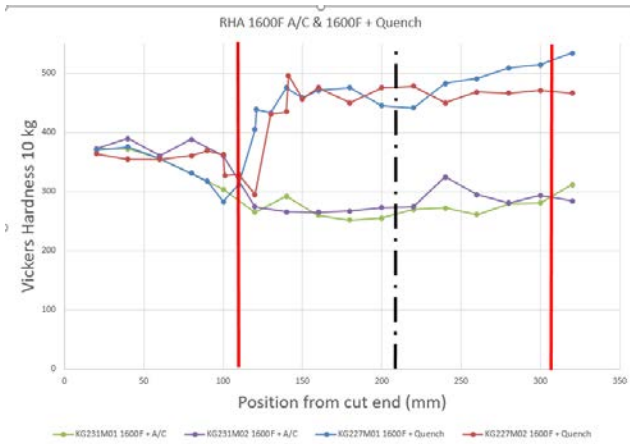


Figure 27: Hardness survey for class 1 RHA plates at 1600°F with and without water quench

For the plates heated to 900°F the hardness is relatively constant at 350 Vickers with the exception of the outboard KG230-M01 macro section where the hardness approaches 300 Vickers at the plate edge.

For the class 1 RHA plates that were heated to 1600°F the results are more divergent with the hardness of the air cooled KG231 dropping close to 250 Vickers and the hardness of the quenched KG227 rising to in excess of 470 Vickers.

The tensile test results for the RHA plates are shown in Table 17.

For the RHA plate air cooled from 900°F (KG230) and the plate quenched from 900°F (KG226) there is little change in the 0.2% proof stress and UTS compared to the parent plate.

For the RHA plate that was air cooled from 1600°F (KG231) there is a significant drop (~60 ksi) in the 0.2% proof stress and ~30 ksi drop in the UTS compared to the parent plate.

For the RHA plate that was water quenched from 1600°F (KG227) the 0.2% proof stress is largely unchanged in the longitudinal direction but drops by ~30 ksi in the transverse direction. The UTS of the same plate is ~50 ksi higher than the parent plate. It should be noted that the 0.2% proof and UTS of the as received class 1 RHA plate are almost identical.

The Charpy impact data for the RHA plates is summarized in Table 6.

Table 6: Charpy impact test results for RHA plates

Rolled Homogenous Armor						
Coupon	Treatment	Coupon Location and Cv -40C (Joules)				
		1	2	5	7	10
Parent	As received					31
KG230	900°F + Air cool	41	37	34	46	35
KG226	900°F + Quench	41	31	38	41	43
KG231	1600°F + Air cool	5	5	5	18	43
KG227	1600°F + Quench	38	34	33	30	41
Location 1 is at the center of the hot zone						
Location 2 is at the center of the hot zone						
Location 5 is approximately on the maximum induction coil oscillation line						
Location 7 is approximately 25mm beyond location 5						
Location 10 is approximately 63mm beyond location 5						

The RHA plate that was air cooled from 1600°F (KG231) has not responded well and the Charpy impact values are poor. The RHA plate that was water quenched from 1600°F has good Charpy impact properties at the measured locations however it is possible that there is a lower toughness zone coincident with the drop in hardness shown in Figure 27 that was not detected with Charpy impact testing due to coupon spacing.

The large system has now been used to apply controlled and localized heat (Figure 28) to 4' wide plates to form bends such as that shown in Figure 29.



Figure 28: Plate being heated locally prior to forming



Figure 29: Plate immediately after forming

Further impact testing and or metallurgical analysis for both “alloy BB and class 1 RHA is recommended to determine the true width of the low toughness zone and thus establish a relationship with hardness and microstructure.

It is considered that the width of this low toughness zone could be further influenced by increasing the applied induction heating power, from the current 35% to near 100%, to determine if the width of the low hardness zone can be reduced as there will be less time for heat conduction and softening before the plate is quenched.

The particular benefit of the higher forming temperature with water quench is that deformation occurs at a lower force resulting in lower residual stresses and there is therefore a lower probability of fractures (real time, delayed or impact related) developing from irregularities at the plate edges. The resultant lower forming loads have the potential to significantly reduce the capital equipment cost required to bend thick armor plate. This project has shown that a 175 ton press is capable of forming a 48” wide bend in 20 mm thick material. A 175 ton brake is significantly cheaper than a 2000 ton press brake even when the cost of the induction system is included.

Conclusion hot forming of Armor steel

For “alloy BB” and class 1 RHA it can be seen that air cooling from 1600°F is detrimental and that processing at 900°F either with or without water quench does not substantially affect the toughness (as measured by charpy impact testing) although it should be noted that there is a drop in the UTS of ~20 to 30 ksi for “alloy BB”.

For the “alloy BB” plate heated to 1600°F and water quenched the mechanical properties are good and equal to those of the parent material with the noted exception of toughness in a band beyond the primary hot zone.

For the class 1 RHA plates heated to 1600°F and water quenched there is an approximately 80 ksi increase in the UTS.

FORMING AND WELDING INNOVATIONS FOR ARMOR STEELS.

John Lawmon et al.

Approved for public release; distribution is unlimited.

Standardized Weldability Testing

It is known that both the RHA and commercial armor are welded with both ferrous and stainless steel weld consumables. Hardness mapping of welds made with and without preheat has shown an average HAZ hardness higher than the critical level required for hydrogen induced cold cracking (HICC) as predicted by the Duren equations. Stainless steel consumables have the potential to “absorb and hold” increased amounts of hydrogen (compared to ferrous consumables) and reduce the residual stress below the critical threshold at which HICC might occur. Schaeffler diagrams were prepared to predict the microstructure and hence first order propensity of each armor weld consumable combination to cracking. These diagrams which are shown in Figure 30 and Figure 31 (Note: The use of the WRC diagram, as opposed to Schaeffler, for the grade 307 (modified) consumable indicates that at 0% dilution there is some ferrite present) suggest that there is a possibility of weld metal cracking when making single pass root welds as summarized in Table 7.

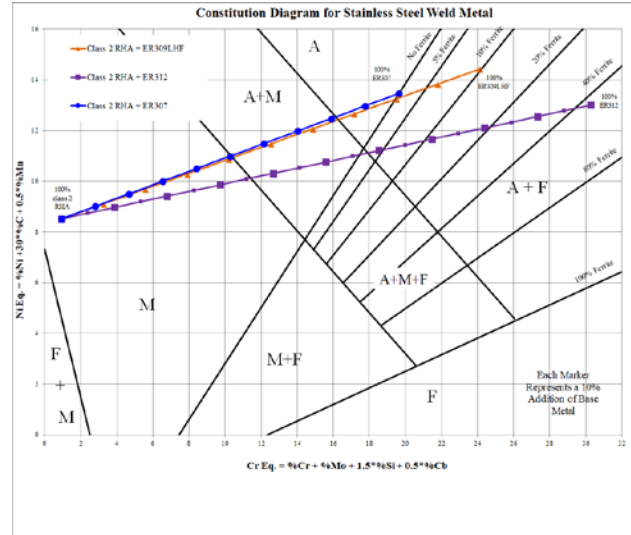


Figure 31: Schaeffler diagram for Class 1 RHA with stainless steel weld metal

Table 7: Potential for weld metal cracking

Base metal	Filler metal	Possible solidification cracking for weld metal dilutions	Possible solidification & or HICC cracking for weld metal dilutions	Possible HICC cracking for weld metal dilutions
Alloy BB	ER307 (modified)	Between 0 & 20%	Between 20 & 50%	Greater than 50%
Alloy BB	ER309	Between 22 & 33% dilution	Between 33 & 58%	Greater than 58%
Alloy BB	ER312	N/A	Between 45 & 64%	Greater than 64%
Class 1 RHA	ER307 (modified)	Between 0 and 19%	Between 19 & 50%	Greater than 50%
Class 1 RHA	ER309	Between 20 and 34%	Between 34 & 58%	Greater than 58%
Class 1 RHA	ER312	N/A	Between 43 & 64%	Greater than 64%

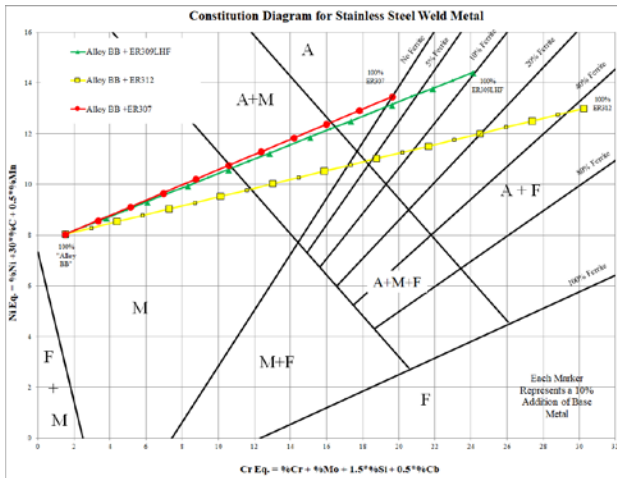


Figure 30: Schaeffler diagram for "Alloy BB" with stainless steel weld metal

To further examine the predictions from the Schaeffler diagrams and rank the propensity of each combination to HICC a program of work was undertaken using standardized testing. The two standardized tests selected were the CTS and Tekken.

The completed setup for the CTS Test [4], [5] is shown in Figure 32 and is comprised of a block, with a deliberately machined notch (Figure 33), bolted to a larger backing plate (Figure 34).

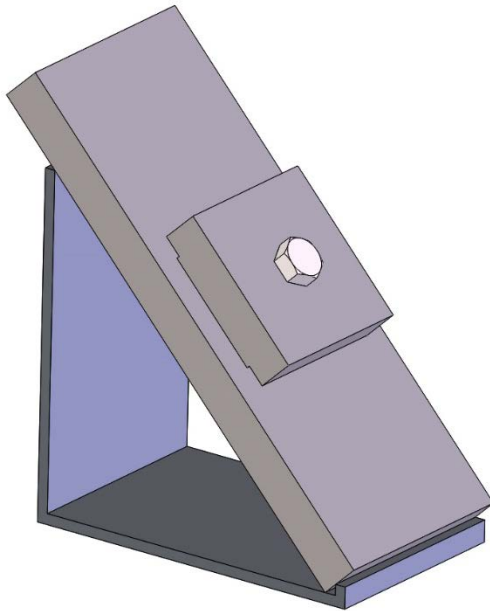


Figure 32: CTS test weld set up without lock welds

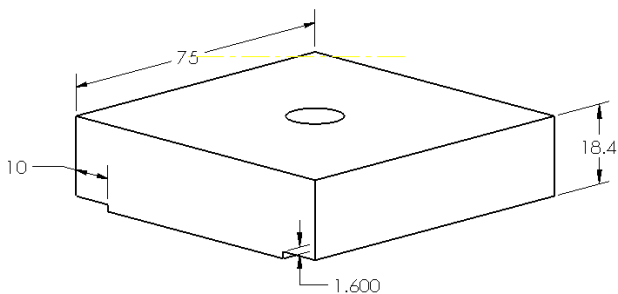


Figure 33: CTS Top block

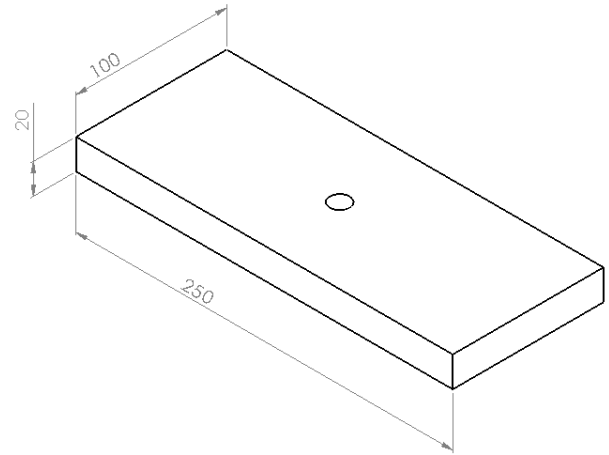


Figure 34: CTS Backing plate

Anchor welds are made between the sides of the blocks and a delay period of at least 12 hours used before making the test welds, over the notch, at the top and bottom of the top block. The standard requires for the lower section of the backing plate to be transferred to a bath of moving water however this was not practiced for this test as it was determined, by plunging a thermocouple into the weld pool, that the cooling time (Figure 35) between T_{8-5} was less than 5 seconds irrespective of the use, or not, of a water quench bath.

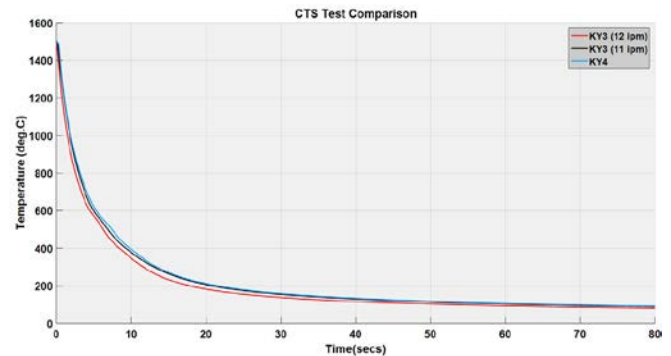


Figure 35: Weld pool cooling times determined by thermocouple plunging

On completion of welding and after a 48 hour soak at temperature the test weld was sectioned (excluding the weld crater area) and analyzed at four locations using macro sections such as those shown in Figure 36 and Figure 37.



Figure 36: Macro section through a CTS weld showing the pre-machined root notch

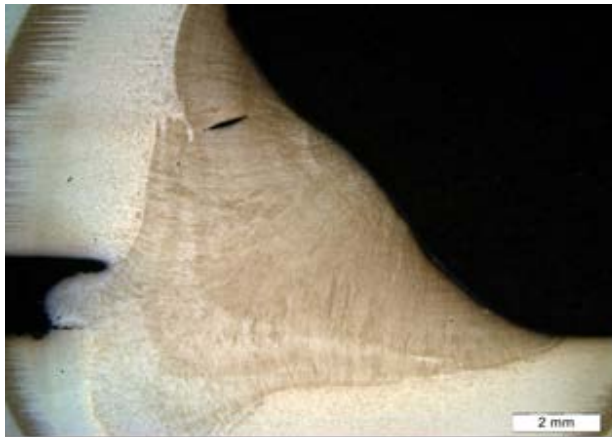


Figure 37: CTS test with crack adjacent to island of parent metal.

The set up for the self-restrained Tekken test is shown in Figure 38 and comprises an 80 mm long central Y groove with a 2 mm root gap.

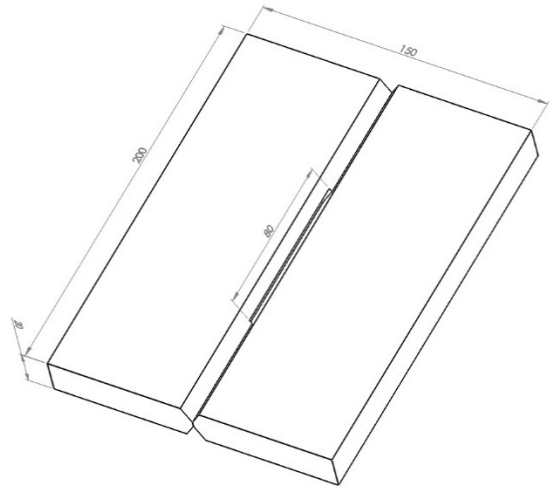


Figure 38: Tekken test piece with 80mm x 2mm central gap

The test pieces used differ from that shown in [4] as they have been deliberately machined to replace the open gap CJP groove weld at either end of the 80 mm Y, which is likely to cause the important 2 mm root gap to collapse, with a double sided PJP groove weld. On completion of the PJP groove weld and a delay of 12 hours the 80mm long test weld was made over the 2mm root gap. This test weld was subsequently sectioned and macro sections, such as those shown in Figure 39 and Figure 40, analyzed at four locations.



Figure 39: Multiple cracks in Tekken test

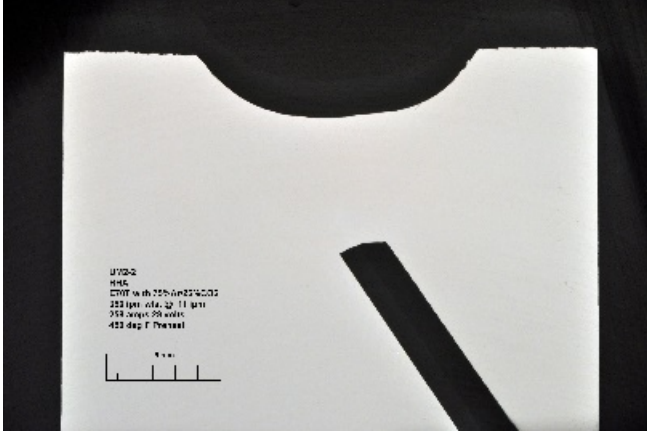


Figure 40: Unetched and crack free Tekken test

Stainless steel weld consumables

Measurements taken from single pass fillet welds have indicated that the weld metal dilution for completely fused welds made with a 98% Ar/2% O₂ gas mixture were in the range of 24 to 36% and with a 90% Ar/10% CO₂ were in the range 36 to 43%.

Weld metal dilution levels recorded in the Tekken and CTS tests are shown in Table 8 and Table 9.

By comparing this data with Table 7 it can be inferred that both solidification cracking and martensitic cracking are possible for all combinations tested.

Table 8: Weld metal dilutions measured in CTS & Tekken tests for "alloy BB"

Base Metal	Weld Consumable	Preheat	Tekken test weld metal dilution	CTS test weld metal dilution
Alloy BB	ER307 (modified)	70°F	44	36
		450°F & PWS	50	40
Alloy BB	ER309LHF	70°F	45	46
		450°F & PWS	45	52
Alloy BB	ER312	70°F	45	41
		450°F & PWS	52	50

Table 9: Weld metal dilutions measured in CTS & Tekken tests for class 1 RHA

Base Metal	Weld Consumable	Preheat	Tekken test weld metal dilution	CTS test weld metal dilution
Class 1 RHA	ER307 (modified)	70°F	66	37
		450°F & PWS	52	46
Class 1 RHA	ER309LHF	70°F	50	45
		450°F & PWS	50	46
Class 1 RHA	ER312	70°F	43	37
		450°F & PWS	48	39

More recent development in thermodynamic simulation have allowed more accurate predictions of phase transformation and these are discussed in detail in [6].

The crack ratio results from both the CTS & Tekken tests made with stainless steel consumables and 90% Ar/10% CO₂ are summarized in Table 10 and Table 11 for "alloy BB" and class 1 RHA. This high percentage of CO₂ was deliberate and selected after making a set of fillet welds in the 1F position to examine fillet weld penetration profiles.

Table 10: CTS & Tekken crack ratio summary for "Alloy BB" welded with stainless steel consumables

Base Metal	Weld Consumable	Preheat	Tekken test results	CTS test results
Alloy BB	ER307 (modified)	70°F	6% Crack ratio	Invalid*
		450°F & PWS	8% Crack ratio	Invalid*
Alloy BB	ER309LHF	70°F	No Cracks	V small WM crack
		450°F & PWS	No Cracks	No Cracks
Alloy BB	ER312	70°F	18% Crack ratio	Invalid*
		450°F & PWS	2% Crack ratio	No Cracks

* The test is invalid as the crack was in the root weld metal and > 5% of throat thickness. The CTS test is for HICC in the HAZ

Table 11: CTS & Tekken crack ration summary for class 1 RHA welded with stainless steel consumables

Base Metal	Weld Consumable	Preheat	Tekken test results	CTS test results
Class 1 RHA	ER307 (modified)	70°F	No cracks	WM < 5%
		450°F & PWS	No cracks	WM < 5%
Class 1 RHA	ER309LHF	70°F	3% Crack ratio	WM < 5%
		450°F & PWS	No cracks	No cracks
Class 1 RHA	ER312	70°F	27% Crack ratio	No cracks
		450°F & PWS	No cracks	No cracks

* The test is invalid as the crack was in the root weld metal and > 5% of throat thickness. The CTS test is for HICC in the HAZ

The stainless steel filler metals that experienced the least severe cracking during Tekken testing were ER309LHF for “alloy BB” and both ER309LHF and ER307 (modified) for class 1 RHA.

The filler metal that experienced the least severe cracking during CTS testing was ER309 in “Alloy BB” and ER312 in class 1 RHA. Many of the CTS test results were deemed invalid per [4] and [5] as the cracks that occurred in the root weld metal exceeded 5 % of the throat size.

All Tekken Test samples which experienced cracking and were welded with a stainless steel consumables cracked in the weld metal as opposed to the heat affected zone (HAZ) and were classed as solidification cracks following metallurgical analysis. According to ISO17642-2 [4] the cracks need to initiate at the stress concentration before they can be classified as initiating as HIC. The absence of HICC could have occurred for one or two of the following reasons: 1. stress was relieved due to the use of a low strength weld consumable and or solidification cracking; 2. hydrogen was absent from the weld and or retained in the austenitic weld metal.

Although the stainless steel weldability tests do not provide definitive data on the susceptibility to HICC, as hydrogen was not measured within the weld metal, the results do provide valuable information. The results show that in highly

restrained conditions, welds produced with the stainless steel filler metals tested are susceptible to solidification cracking with the exception of:

- “Alloy BB” welded with ER309LHF either with or without preheat.
- Class 1 RHA welded with preheat with either ER309LHF or ER312.

A complimentary set of 1” and 7” long single sided T fillet welds (with low restraint) was made, and subsequently metallurgically examined, using both 90% Ar/10% CO₂ and 98% Ar/2% O₂ shielding gases without and with preheat to examine the sensitivity of “alloy BB” and class 1 RHA to solidification cracking in a nominally free state with different fusion profiles. The results of the metallurgical analysis [9] (Table 12) show that no cracks were found when welding “alloy BB” with any of the three stainless steel consumables and gas combinations. The results (Table 13) [9] of welding class 1 RHA with the same three stainless steel consumables and gas combinations show that grade 312 is the only consumable that has not cracked and it is suspected that the crack noted with grade 307 (modified) is a crater crack. The reason for the large solidification crack associated with the ER309LHF/90% Ar/10% CO₂/no-preheat combination is not known.

Table 12: Cracking incidence for "alloy BB" fillet welds made with different weld consumables, shield gas and preheat levels

Base metal & filler metal	No preheat and 90% Ar/10% CO ₂	Preheat and 90% Ar/10% CO ₂	No preheat and 98% Ar/2% O ₂	Preheat and 98% Ar/2% O ₂
“Alloy BB” & ER307 (modified)	No cracks	No cracks	No cracks	No cracks
“Alloy BB” & 309LHF	No cracks	No cracks	No cracks	No cracks
“Alloy BB” & ER312	No cracks	No cracks	No cracks	No cracks

Table 13: Cracking incidence for "class 1 RHA" fillet welds made with different weld consumables, shield gas and preheat levels

Base metal & filler metal	No preheat and 90% Ar/10% CO ₂	Preheat and 90% Ar/10% CO ₂	No preheat and 98% Ar/2% O ₂	Preheat and 98% Ar/2% O ₂
"Class 1 RHA" & ER307 (modified)	One – may be in weld crater	No cracks	No cracks	No cracks
"Class 1 RHA" & 309LHF	Cracked in 7" weld	No cracks	No cracks	No cracks
"Class 1 RHA" & ER312	No cracks	No cracks	No cracks	No cracks

Ferrous weld consumables

The results from both the CTS & Tekken tests made with ferrous consumables are summarized in Table 14 and Table 15 for "alloy BB" and class 1 RHA.

Table 14: CTS & Tekken analysis summary for Alloy BB made with ferrous consumables

Base Metal	Weld Consumable	Preheat	Tekken Test Results	CTS Test Results
Alloy BB	ER70S-6	70°F	100% Crack ratio	Invalid*
		450°F & PWS	8% Crack ratio	Invalid*
Alloy BB	ER100	70°F	100% Crack ratio	No Cracks
		450°F & PWS	No Cracks	No Cracks

* The test is invalid as the crack was in the root weld metal and > 5% of throat thickness. The CTS test is for HICC in the HAZ

Table 15: CTS & Tekken analysis summary for class 1 RHA made with ferrous consumables

Base Metal	Weld Consumable	Preheat	Tekken Test Results	CTS Test Results
Class 1 RHA	ER70S-6	70°F	100% Crack ratio	Invalid*
		450°F & PWS	8% Crack ratio	Invalid*
Class 1 RHA	ER100	70°F	100% Crack ratio	Invalid*
		450°F & PWS	No cracks	Invalid*

* The test is invalid as the crack was in the root weld metal and > 5% of throat thickness. The CTS test is for HICC in the HAZ

From both the Tekken & CTS weldability test results it can be seen that ER70S-6 and LA100 filler metals are susceptible to cracking in the weld metal. Figure 41 shows examples of the fracture faces (for both ER70S-6 and LA100 welds) of cracks that were observed along solidification grain boundaries. The fracture surfaces of these cracks revealed liquid along the fracture surface, leading to the conclusion that these were solidification cracks. These CTS solidification weld metal cracks were observed adjacent to a weld metal swirl (shown in Figure 41C) and located close to the fusion boundary associated with the top rectangular block as shown in Figure 42. (The stainless steel

weld metal cracks were found in the middle of the weld). The weld swirls were found to have very high hardness' (460 Hv to 510 Hv for "alloy BB" and 570 to 610 for class 1 RHA) and it is thought that upon final solidification of the weld metal that they are points of high restraint and potential initiators for solidification cracking. Testing of weldments made at room temperature and 450°F showed that the HAZ hardness of "alloy BB" and class2 RHA fillet welds was unaffected by preheat.

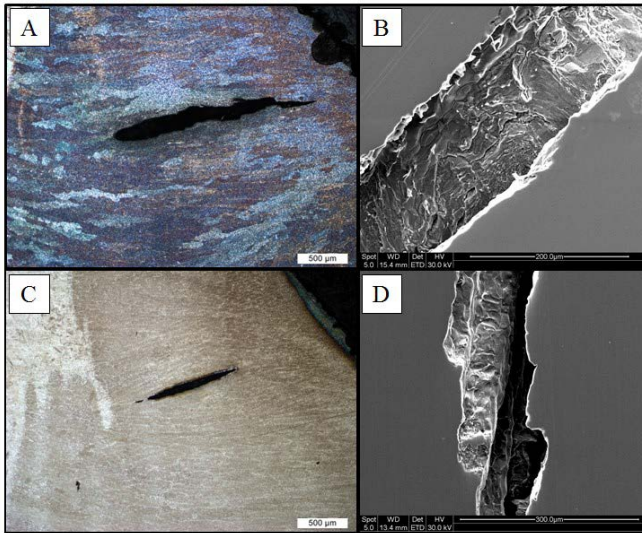


Figure 41: [A] RHA + ER70S-6 (No Preheat) WM crack [B] Fracture surface of RHA + ER70S-6 (No Preheat) WM crack [C] RHA + ER100 (Preheat) WM crack [D] Fracture surface of RHA + ER100 (Preheat) WM crack

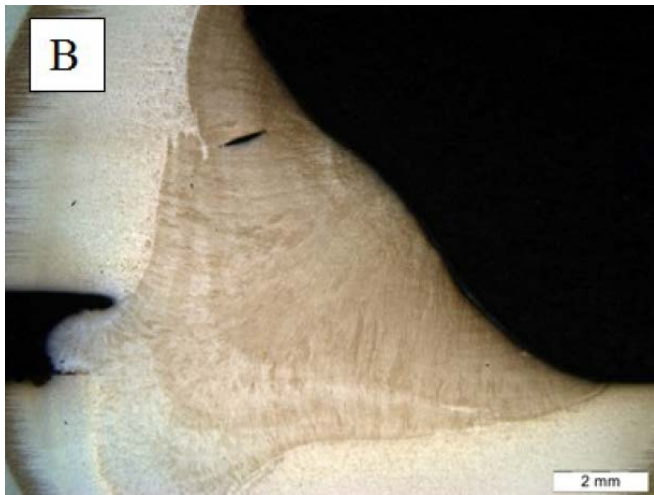


Figure 42: CTS weld made with LA100 and class 1 RHA showing solidification crack adjacent to side wall weld metal swirl

Both room temperature Tekken test welds made with ER70S-6 and ER100 cracked through the entire weld (crack section ratio = 100%). The fracture surface of the crack changed as the crack propagated as shown in Figure 43.

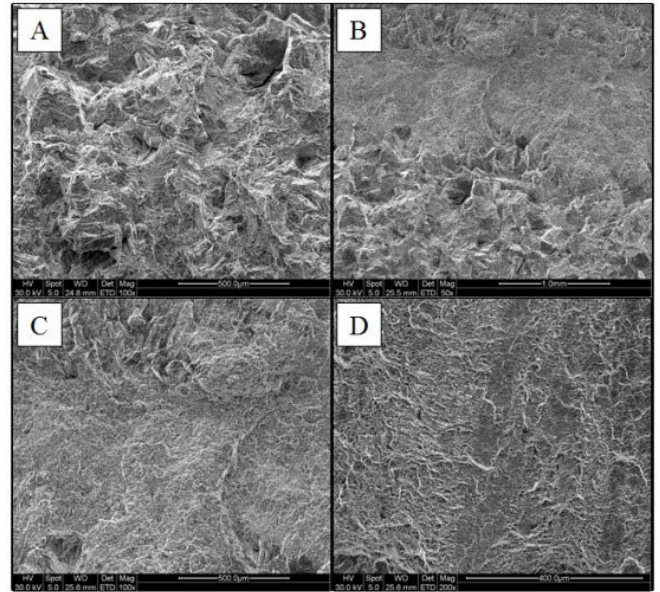


Figure 43: Crack Fracture Surface Change in "alloy BB" + ER70S-6 [A] Intergranular [B] Intergranular transitioning to quasi-cleavage at the fusion boundary [C] Quasi-cleavage near the weld swirl [D] Microvoid Coalescence in the WM

The fracture surface was intergranular in the HAZ (Figure 43A), then adjusted to a cleavage surface (Figure 43B and C), and, finally, the crack ended with a ductile surface (Figure 43D). The change in fracture surface indicates that this weld experienced some HICC [7].

In both the CTS and Tekken Tests with ER70S-6 and LA100 the application of preheat reduced the severity of the cracking for both "alloy BB" and class 1 RHA. It is likely that the application of preheat allows the diffusion of hydrogen, and minimizes the thermal gradient in the HAZ which reduces the restraint developed in the solidifying test weld.

Except for the CTS weld made with ER100 and "alloy BB", which did not crack at all, the CTS Tests were considered "invalid" because the cracks were located in the weld metal and the crack

FORMING AND WELDING INNOVATIONS FOR ARMOR STEELS.

John Lawmon et al.

Approved for public release; distribution is unlimited.

lengths exceeded 5% of the throat thickness. it is therefore considered likely that the Tekken test is a more suitable test for HICC with these combinations.

consumable cracked less than the more ductile lower strength ER70S-6.

Conclusion - weldability testing

The relatively unrestrained fillet welds were crack free with the exception of one grade 309LHF weld made without preheat with class 1 RHA.

All CTS and Tekken test weld metal cracks were confirmed to be solidification cracks because they occurred along solidification grain boundaries and exhibited a dendritic fracture surface morphology. Although many of the CTS Tests were considered "invalid", the CTS results imply that under the high restraint, there is a potential for solidification cracking when welding both armored steels with stainless steel filler metals. The extent of cracking was minimized by preheating the joint prior to welding.

The data suggests that ER309LHF which experienced little to no cracking compared to the other stainless steels consumables is the most suitable for welding "alloy BB" and that more research is required before a similar conclusion can be reached for class 1 RHA when a single pass weld is used.

As little to no delta ferrite is retained in the weld metal for the observed dilutions it is important to carefully manage the weldment to minimize phosphorus, sulfur and to some extent silicon levels to minimize the possibility of solidification cracking.

It is recommended that this work be supplemented with multi pass welds, higher heat input welds (potentially vertically up), lower travel speeds to modify weld bead shape and additional restrained joints such as the T joint solidification cracking test (setup type C) detailed in [8].

The application of preheat significantly reduces the incidence of cracking in the heat affected zone when using ferrous consumables and contrary to expectations the higher strength LA100 weld

REFERENCES

- [1] Gerald Lutjering & J Williams. Titanium. Published by Springer.
- [2] MSc thesis by Nick Kulman. The Ohio State University. Metallurgical Characterization of Armor Alloys for the Development and Optimization of Induction Bending Procedures.
- [3] MSc thesis by Tiffany Ngan. The Ohio State University. Evaluation of the Response of Armor Alloys to High Temperature Deformation.
- [4] ISO 17642-2 Destructive tests on welds in metallic materials – Cold cracking tests for weldments - Arc welding processes – Part 2: Self restraint tests.
- [5] AWS B4.0M Standard method for mechanical testing of welds.
- [6] MSc thesis by Matthew Duffey. Metallurgical characterization and weldability evaluation of ferritic and austenitic welds in armor steels. The Ohio State University.
- [7] Beachem, C. D. (1972). A new model for hydrogen-assisted cracking (hydrogen “embrittlement”). Metallurgical transactions, 3(2), 441-455.
- [8] ISO 17641-2-2005 Destructive tests on welds in metallic materials – Hot cracking tests for weldments – arc welding processes.
- [9] AEM review by John Lawmon on the single pass fillet welding of armor steels with and without preheat using 90% Ar/10% CO₂ and 98% Ar/2% O₂ shield gas.

Table 16: Tensile test results for "Alloy BB" plates

"Alloy BB"						
Coupon	Condition	0.2% Offset (ksi)	UTS (ksi)	Elongation (%)	Reduction of area (%)	
Parent Material "Alloy BB"	As received	168	208			
KG172LT001 (edge)	900°F + Air cool	155	167	17.2	63	
KG172LT002 in a bit	900°F + Air cool	163	178	14.3	61.3	
KG172LT003 across edge of weave	900°F + Air cool	170	186	13.3	61.7	
KG172TT004 transverse center of hot zone	900°F + Air cool	165	179	14.3	61	
KG232LT002	900°F + Air cool	163	174	15.2	63.5	
KG232TT004	900°F + Air cool	163	173	13.2	59.6	
KG223LT002	900°F + Quench	169	182	13.7	59	
KG223TT004	900°F + Quench	168	181	13.9	59.4	
KG171LT001 (edge)	1600°F + Air cool	112	154	17.3	60.6	
KG171LT002 in a bit	1600°F + Air cool	116	164	18.3	59.4	
KG171LT003 across edge of weave	1600°F + Air cool	123	149	10.7	59.6	
KG171TT004 transverse center of hot zone	1600°F + Air cool	119	164	15.4	55	
KG233LT002	1600°F + Air cool	115	163	16.9	57.2	
KG233TT004	1600°F + Air cool	118	162	14	53.4	
KG222LT002	1600°F + Quench	157	218	15.2	58.7	
KG222TT004	1600°F + Quench	158	220	14.5	53.7	

FORMING AND WELDING INNOVATIONS FOR ARMOR STEELS.

John Lawmon et al.

Approved for public release; distribution is unlimited.

Table 17: Tensile test results for class 1 RHA plates

Class 1 Rolled Homogenous Armor					
Coupon	Condition	0.2% Offset (ksi)	UTS (ksi)	Elongation (%)	Reduction of area (%)
Parent material class 1 RHA	As received	162	169	14.7	58.5
KG230LT002	900°F + Air cool	165	173	14.8	58.1
KG230TT004	900°F + Air cool	164	172	12.6	52.6
KG226LT002	900°F + Quench	167	174	13.3	56.8
KG226TT004	900°F + Quench	165	173	13.5	52.2
KG231LT002	1600°F + Air cool	97.5	143	15.1	51
KG231TT004	1600°F + Air cool	98.5	141	15.1	46.5
KG231TT003	1600°F + Air cool	104	131	12.5	51.5
KG227LT002	1600°F + Quench	173	247	12.9	48.7
KG227TT004	1600°F + Quench	171	247	11.6	40.6
KG227TT003	1600°F + Quench	130	143	10.9	58.8

FORMING AND WELDING INNOVATIONS FOR ARMOR STEELS.

John Lawmon et al.

Approved for public release; distribution is unlimited.